Demonstration of superconducting micromachined cavities

T. Brecht, M. Reagor, Y. Chu, W. Pfaff, C. Wang, L. Frunzio, M. H. Devoret, and R. J. Schoelkopf

---

Articles you may be interested in

Coupling of a locally implanted rare-earth ion ensemble to a superconducting micro-resonator
Appl. Phys. Lett. **105**, 102601 (2014); 10.1063/1.4894455

In-situ scanning electron microscopy and atomic force microscopy Young's modulus determination of indium oxide microrods for micromechanical resonator applications
Appl. Phys. Lett. **104**, 161909 (2014); 10.1063/1.4872461

Reaching 10 ms single photon lifetimes for superconducting aluminum cavities
Appl. Phys. Lett. **102**, 192604 (2013); 10.1063/1.4807015

Improving the performance of superconducting microwave resonators in magnetic fields
Appl. Phys. Lett. **98**, 102504 (2011); 10.1063/1.3560480

Results of Q Disease Tests With 350-MHz Spoke Cavities
AIP Conf. Proc. **671**, 220 (2003); 10.1063/1.1597370

Demonstration of superconducting micromachined cavities

T. Brecht,[a] M. Reagor, Y. Chu, W. Pfaff, C. Wang, L. Frunzio, M. H. Devoret, and R. J. Schoelkopf
Department of Applied Physics, Yale University, New Haven, Connecticut 06511, USA

Superconducting enclosures will be key components of scalable quantum computing devices based on circuit quantum electrodynamics. Within a densely integrated device, they can protect qubits from noise and serve as quantum memory units. Whether constructed by machining bulk pieces of metal or microfabricating wafers, 3D enclosures are typically assembled from two or more parts. The resulting seams potentially dissipate crossing currents and limit performance. In this letter, we present measured quality factors of superconducting cavity resonators of several materials, dimensions, and seam locations. We observe that superconducting indium can be a low-loss RF conductor and form low-loss seams. Leveraging this, we create a superconducting micromachined resonator with indium that has a quality factor of two million, despite a greatly reduced mode volume. Inter-layer coupling to this type of resonator is achieved by an aperture located under a planar transmission line. The described techniques demonstrate a proof-of-principle for multilayer microwave integrated quantum circuits for scalable quantum computing. © 2015 AIP Publishing LLC.
[http://dx.doi.org/10.1063/1.4935541]

Quantum information devices based on the circuit quantum electrodynamics (cQED) platform are now reaching a level of complexity that demands careful attention to the challenges of connectorization, addressability, and isolation of constituent components. Solutions will ideally allow for dense packing of components and routing of control and readout circuitry, while protecting the coherence of quantum states and maintaining the performance of numerous integrated elements.

The semiconductor industry has already solved similar challenges in the classical domain. An exciting prospect is adapting these known methods of 3D integration and packaging for RF components[1] to scale-up quantum circuits. We envision using micromachining, the bulk etching of silicon wafers, to embed cQED components within a multi-wafer construction (Fig. 1(a)) containing many superconducting qubits, memories, buses, and amplifiers. Therefore, we have proposed a hardware platform called the multi-layer microwave integrated quantum circuit (MMIQC).[2,3] Micromachined enclosures, which have been demonstrated in normal metal RF circuitry,[4,5] are highly useful in such a device stack if extended to superconducting coatings. They can suppress cross-talk and radiation loss in circuits, or constitute cavity resonators that can serve as quantum memories. Both applications will require 3D superconducting enclosures that are very low-loss, despite highly confined electric fields and surface currents.

In this letter, we show that it is crucial to achieve a superconducting bond between the micromachined layers in order to achieve a low-loss enclosure. Further, we demonstrate that indium can fulfill this objective. We first describe a model that allows us to quantify the dissipation that a seam introduces to a cavity mode. We then present measurements of traditionally machined cavity resonators with several

materials, dimensions, and seam locations chosen to elucidate the seam as a loss mechanism. These measurements reveal that indium can yield high quality factors ($Q_{int} = 8 \times 10^7$) and form a superconducting bond for various types of enclosures. Combining this finding with established fabrication techniques, we have created superconducting micromachined cavities. As we describe, such devices are particularly susceptible to loss at seams, but with indium, they can achieve quality factors of up to two million. They can also be coupled with planar techniques, making them compatible with future multi-wafer stacks containing cQED experiments.
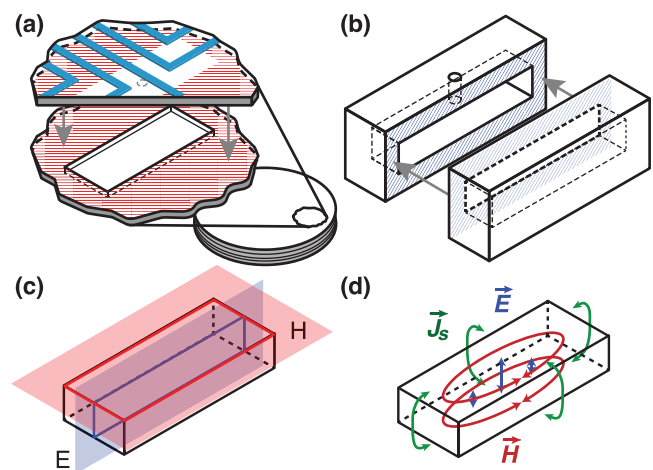

FIG. 1. Seam locations in rectangular cavities. (a) A micromachined cavity formed between two wafers. By coupling to a planar transmission line from an adjacent layer, this unit is suitable for integration in a multilayer microwave integrated circuit. Compared to (b), the height of the cavity is reduced by a factor of 10 and the seam has perpendicular orientation. (b) Cavity used in some cQED experiments.[6] In (a) and (b), surfaces that meet to form a seam are patterned with red and blue lines. (c) Seam locations in the rectangular cavity are shown by cuts in planes H and E. (d) Electric (blue) and magnetic (red) field lines of the TE101 mode, and the corresponding surface currents (green).

[a]Electronic mail: teresa.brecht@yale.edu

In addition to dielectric and conductor losses,[7–11] a cavity assembled from two conductors can experience loss from an imperfect seam.[12–15] Currents crossing the joint between two superconducting walls encounter a discontinuity due to microscopic voids, oxides, or other surface impurities. Therefore, the types of cavities that are commonly used in cQED experiments[6] are designed to mitigate seam losses (Fig. 1(b)). These cavities are assembled from two symmetric halves, split along a plane E shown in Fig. 1(c). The cavity's TE_{n0m} modes ideally have no currents crossing the seam for this configuration (Fig. 1(d)). Other cavity resonators that have this property include the TE_{011} mode of a cylindrical cavity,[11,16] coaxial quarter-wave cavities,[17] as well as cavities constructed by extruding methods, such as hydroforming. However, none of these cavity constructions are practical for wafer-processing. MMIQCs' constitutive micromachined enclosures (Fig. 1(a)) are etched into silicon wafers and have seams that experience large currents: those parallel to plane H in Figure 1(c).

We now quantify the dependence of seam losses on the cavity geometry. We model the seam as a distributed port around a path $\vec{l}$ with a total length L and total conductance G_{seam}. The cavity fields are accompanied by surface currents $\vec{J}_s$ that may pass across the seam and dissipate power

$$P_{dis} = \frac{1}{2G_{seam}} L \int_{seam} |\vec{J}_s \times \hat{l}|^2 dl. \qquad (1)$$

If it is damped solely by seam losses, a cavity mode of frequency ω and total energy E_{tot} has a quality factor Q_i given by

$$\frac{1}{Q_i} = \frac{1}{\omega} \frac{P_{dis}}{E_{tot}} = \frac{1}{G_{seam}} \left[\frac{L \int_{seam} |\vec{J}_s \times \hat{l}|^2 dl}{\omega \mu_o \int_{tot} |\vec{H}|^2 dV} \right] = \frac{y_{seam}}{g_{seam}}, \qquad (2)$$

where the field $\vec{H}$ is integrated over the volume V of the mode and μ_o is the magnetic permeability. We identify the expression in square brackets as the admittance, Y_{seam}, of the cavity presented to the seam. This admittance is zero when the seam is placed such that there are no perpendicular surface currents. In order to compare intrinsic seam properties in different cavity constructions, we introduce the conductance per unit length $g_{seam} = G_{seam}/L$ and admittance per unit length $y_{seam} = Y_{seam}/L$. Using this model, we can associate y_{seam} with the seam location and cavity fields and g_{seam} with materials properties in the seam region.

From these equations and the known fields of the TE_{101} mode (Fig. 1(d)), we see that plane H of Figure 1(c) maximizes y_{seam}. However, this seam orientation is the natural consequence of the micromachining process.[5] Therefore, for a low-loss micromachined cavity, it is imperative to develop a method of wafer-scale superconducting bonding that maximizes g_{seam}. By measuring several seam-limited quality factors, we can extract values of g_{seam} for cavities bonded using different materials and techniques.

Fig. 2 presents several measurements of quality factors for rectangular waveguide cavity resonators. These devices were machined in bulk metal to various geometries, and assembled with several seam locations to study the effect of varying y_{seam}. Moreover, various materials were used: 6061
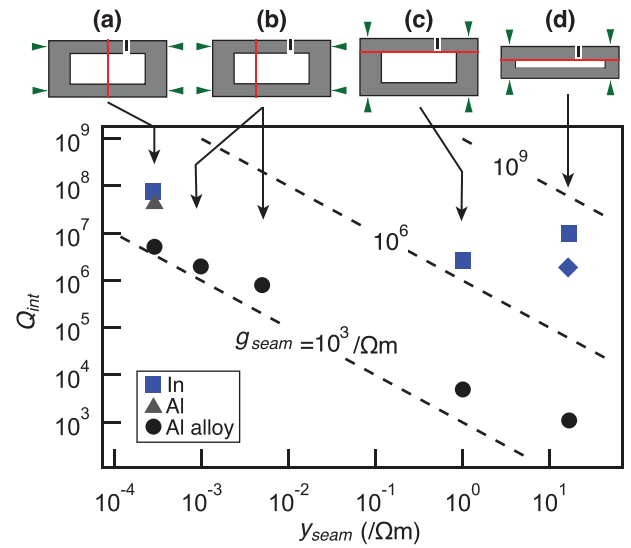

FIG. 2. Quality factor measurements of Al and In cavities. Internal quality factors of cavity resonators plotted against seam admittance. Each y_{seam} is calculated using the known fields of the cavity geometry and a seam path. Black dashed lines correspond to several g_{seam} values. (a)–(d) Pictorial descriptions show a transverse plane cross-section of several cavity constructions. Dimensions of cavities of types (a)–(c) were approximately $33 \times 18 \times 5$ mm. The dimensions of cavity type (d) were $28 \times 19 \times 0.3$ mm and $22 \times 24 \times 0.3$ mm. All cavities were coupled using a pin in a sub-cutoff waveguide and had TE101 resonances between 9.45 and 9.54 GHz. Measurements were taken in hanger configuration at temperatures of about 20 mK. With the exception of the diamond point, the two halves of all the cavities were bolted together with four screws that remained during measurement, applying force indicated by green arrows. We plot one In-plated micromachined cavity in Si bonded to In-plated Cu without the use of screws or clamping (blue diamond).

aluminum alloy (black circles), aluminum of $>4N$ purity (grey triangle), or electroplated indium (blue squares/diamond), to study how material choices contribute to g_{seam}. In the following, we describe the cavities in order of increasing seam participation.

We begin with a rectangular cavity geometry similar to those used in 3D cQED experiments,[6] assembled in two halves that meet at a seam in plane E (Figs. 1(b), 1(c), and 2(a)). Machining imprecision of ± 2 mils may cause deviation from the ideal $y_{seam} = 0$. In bulk Al, these cavities typically have $Q_{int} = 10^6$–10^7. Pure ($>4N$) Al cavities, when chemically etched, have higher Q_{int} due to reduced surface loss. The same cavity geometry was also machined in OFHC Cu and electroplated with In to a thickness of $100 \, \mu m$ before assembly. The resulting quality factor of 8×10^7 exceeded that of the Al 4N cavity. Our cavity measurements place a bound on indium's surface quality, described in Ref. 7 as the ratio of a superconductor's surface reactance to surface resistance, of $Q_S > 3 \times 10^3$.

Next, we describe measurements performed on rectangular cavities with seam participation intentionally increased. We machined the mating parts in Al alloy to have either a 5% or 10% asymmetry along their length such that, once assembled, the E-plane seam was not centered (Fig. 2(b)). The increased y_{seam} is accompanied by 60% and 85% reductions in Q_{int} compared to the cavity with symmetric E-plane seam. We also constructed cavities of similar dimensions with seams in the H-plane (Fig. 2(c)). Al cavities with H-plane seams (Fig. 2(c)) had quality factors limited to

5×10^3. In an identical geometry, we observe that cavities constructed from Cu components electroplated with In had quality factors of three orders of magnitude greater ($Q_{int} = 2.7 \times 10^6$).

The cavities with the most seam participation, located on the right side of Figure 2, are metal cavities made with a height of 300 μm, which is feasible to micromachine in a wafer (Fig. 2(d)). In addition to the discussed sensitivity to seam losses, these thin cavities are also more sensitive to surface and conductor losses when compared to larger cavities, with participation ratios scaling inversely with cavity height. It is clear from our measurements, however, that the dominant loss mechanism for these Al cavities is related to the seam.

We conclude that the In-plated Cu cavities have a g_{seam} far exceeding that of the Al cavities. Taking $g_{seam} = 10^4/\Omega$m as a likely limit for the Al alloy cavities, this implies an average total conductance of the seams of these cavities of $G_{seam} = 1/[1.25 \, \mu\Omega]$. However, the measured In cavities with equal y_{seam} possess a higher conductance $g_{seam} = 10^8/\Omega$m, meaning that the total conductance of an In seam cavity can be at least as high as $G_{seam} = 1/[70 \, n\Omega]$. We attribute this difference to a comparably weak surface oxide. Another factor may be indium's higher ductility, which is maintained at cryogenic temperatures.[18] In addition to enhanced seam quality, these measurements also indicate that thick In film has a high surface quality.

Having explored the properties of electroplated indium as a superconducting bonding material using metallic prototypes, we now turn to cavities fabricated in wafers. Compatible with MMIQCs, silicon wafers are etched to form recesses, which are then electroplated with indium to form cavities. Details of the fabrication process are described in Ref. 20.

For initial testing, an In-plated Si chip with etched cavity pit was bonded to a block of In-plated Cu containing a sub-cutoff waveguide for pin coupling in a manner identical to the 3D cavities machined in bulk metal. This bond provided both the mechanical and electrical integrity of the micromachined cavity construction, and can result in a Q_{int} exceeding 10^6 (Fig. 2, blue diamond).

A coupling scheme that is more compatible with a multilayer architecture is achieved using a coplanar waveguide or microstrip to access the fields of the resonator through an aperture in the cavity wall, as described in Refs. 4, 5, and 20. In Fig. 3, we present a superconducting micromachined cavity with planar coupling, consisting of an etched cavity mated with a printed circuit board (PCB) top chip. Of the several devices with various designed couplings,[20] we report a best Q_{int} of 4.6×10^5 ($Q_c = 1.4 \times 10^5$).

Though it exceeds what could be achieved for an Al coating, this result is inconsistent with quality factors shown to be possible in this geometry, and we attribute it to seam loss. We suspect that there is both an oxide barrier and voids in the seam due to imperfect indium electroplating and a non-optimized bonding procedure. Furthermore, we suspect that the integrity of the bonds suffers from a mismatch in the thermal contraction of different materials that we do not expect in future multilayer Si devices.

From this investigation, we conclude that while micromachined cavities are sensitive to seam losses, high-quality
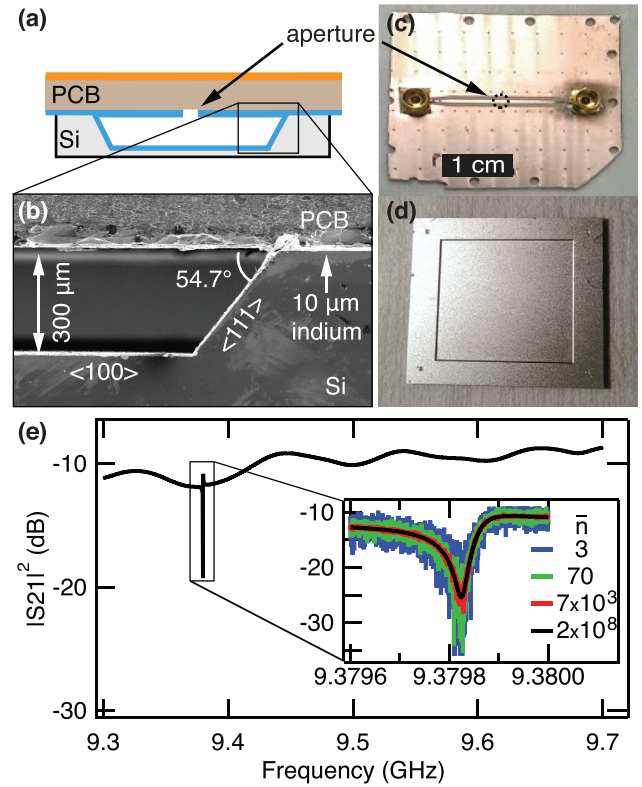

FIG. 3. Superconducting micromachined cavity. (a) Sketch of a transverse plane cross-section of the device. (b) SEM of a cross-section of the device. (c) The top chip is made in TMM10i PCB and contains Cu plated vias and 10 μm In is electroplated on the back side. An aperture (dashed circle, r = 675 μm) is omitted in the back side metallization to permit coupling of cavity fields through the dielectric to the CPW trace above. (d) The bottom chip consists of a 22×24 mm rectangular pit wet etched in a 1 mm thick Si wafer and coated in 100 nm evaporated Cu before electroplating with 10 μm In. (e) A 500 MHz range of the transmission spectrum of the device shows the TE101 resonance. Measured at 20 mK and 7×10^3 photons, a fit to the asymmetric lineshape[19] yields $Q_{int} = 4.6 \times 10^5$ and $Q_c = 1.4 \times 10^5$.

superconducting bonds are possible with the proper selection and treatment of materials. Our results suggest that indium is a low loss ($Q_S > 3 \times 10^3$) and viable superconducting bonding material for a multilayer cQED hardware platform. This bond quality ($g_{seam} = 10^8/\Omega$m) could likely be improved significantly by incorporating techniques such as surface passivation, heating, and precise alignment, which are standard in industrial bump bonding.[21,22] The RF loss properties of superconducting interconnects and wafer-scale bonds produced with these techniques[23] is a topic of current investigation.

Micromachining cavity resonators with the process described here offers the advantages of lithographic precision and ease of integration with planar circuitry. We have demonstrated the planar fabrication of inter-layer coupling to a micromachined cavity. Similar RF interconnects can mediate couplings in an indium bonded stack of silicon wafers with multiple resonators and other quasi-3D and planar elements.[1] The micromachined device presented here is an important step towards developing fabrication strategies necessary for scalable quantum computing.[2]

[1]L. P. B. Katehi, J. F. Harvey, and K. J. Herrick, IEEE Microwave Mag. **2**, 30 (2001).

[2]T. Brecht, W. Pfaff, Y. Chu, L. Frunzio, M. H. Devoret, and R. J. Schoelkopf, e-print arXiv:1509.01127.

[3]R. J. Schoelkopf, T. Brecht, L. Frunzio, and M. Devoret, WO patent application PCT/US2014/012,073 (2014).

[4]L. Harle, "Microwave micromachined cavity filters," Ph.D. thesis (University of Michigan, 2003).

[5]A. R. Brown, P. Blondy, and G. M. Rebeiz, Int. J. RF Microwave Comput. Aided Eng. **9**, 326–337 (1999).

[6]H. Paik, D. I. Schuster, L. S. Bishop, G. Kirchmair, G. Catelani, A. P. Sears, B. R. Johnson, M. J. Reagor, L. Frunzio, L. I. Glazman, S. M. Girvin, M. H. Devoret, and R. J. Schoelkopf, Phys. Rev. Lett. **107**, 240501 (2011).

[7]J. Zmuidzinas, Annu. Rev. Condens. Matter Phys. **3**, 169 (2012).

[8]K. Geerlings, S. Shankar, E. Edwards, L. Frunzio, R. Schoelkopf, and M. Devoret, Appl. Phys. Lett. **100**, 192601 (2012).

[9]J. Gao, J. Zmuidzinas, B. A. Mazin, P. K. Day, and H. G. Leduc, Nucl. Instrum. Methods Phys. Res., Sect. A **559**, 585 (2006).

[10]J. Wenner, R. Barends, R. C. Bialczak, Y. Chen, J. Kelly, E. Lucero, M. Mariantoni, A. Megrant, P. J. J. O'Malley, D. Sank *et al.*, Appl. Phys. Lett. **99**, 113513 (2011).

[11]M. Reagor, H. Paik, G. Catelani, L. Sun, C. Axline, E. Holland, I. M. Pop, N. A. Masluk, T. Brecht, L. Frunzio *et al.*, Appl. Phys. Lett. **102**, 192604 (2013).

[12]W. Singer, X. Singer, S. Aderhold, A. Ermakov, K. Twarowski, R. Crooks, M. Hoss, F. Schölz, and B. Spaniol, Phys. Rev. Spec. Top.-Accel. Beams **14**, 050702 (2011).

[13]A. F. Harvey, Proc. IEE - Part B **102**, 493–499 (1955).

[14]J. Hesler, IEEE MTT-S **2**, 783–786 (2001).

[15]S. Kuhr, S. Gleyzes, C. Guerlin, J. Bernu, U. B. Hoff, S. Deléglise, S. Osnaghi, M. Brune, J.-M. Raimond, S. Haroche, E. Jacques, P. Bosland, and B. Visentin, Appl. Phys. Lett. **90**, 164101 (2007).

[16]J. P. Turneaure and I. Weissman, J. Appl. Phys. **39**, 4417 (1968).

[17]M. Reagor, W. Pfaff, C. Axline, R. W. Heeres, N. Ofek, K. Sliwa, E. Holland, C. Wang, J. Blumoff, K. Chou *et al.*, e-print arXiv:1508.05882v2.

[18]R. P. Reed, C. N. McCowan, R. P. Walsh, L. A. Delgado, and J. D. McColskey, Mater. Sci. Eng. A **102**, 227 (1988).

[19]M. S. Khalil, M. J. A. Stoutimore, F. C. Wellstood, and K. D. Osborn, J. Appl. Phys. **111**, 054510 (2012).

[20]See supplementary material at http://dx.doi.org/10.1063/1.4935541 for details of machined cavity constructions, fabrication methods for micromachined cavities, and additional measurements of micromachined cavities with planar coupling.

[21]Q. Huang, G. Xu, G. Quan, Y. Yuan, and L. Luo, J. Semicond. **31**, 116004 (2010).

[22]C. Broennimann, F. Glaus, J. Gobrecht, S. Heising, M. Horisberger, R. Horisberger, H. C. Kästli, J. Lehmann, T. Rohe, and S. Streuli, Nucl. Instrum. Methods Phys. Res., Sect. A **565**, 303 (2006).

[23]T. M. Miller, C. A. Jhabvala, E. Leong, N. P. Costen, E. Sharp, T. Adachi, and D. J. Benford, Proc. SPIE **8453**, 84532H (2012).